Studies On the Rheological Behavior of High-Impact Polystyrene Prepolymerizing Systems

(SONG ZHIQIANG, YUAN HUIGEN, and PEN ZUREN, *Chemical Engineering Department, Zhejiang University, Hangzhou, China*

Synopsis

The rheological behavior of high-impact polystyrene prepolymer and its two phases separated by ultracentrifugation was studied. The viscosities of prepolymer, polystyrene phase, and rubber phase were correlated with various parameters, and a quantitative relationship among these three viscosities was proposed.

INTRODUCTION

High-impact polystyrene (HIPS) is a reinforced plastic commercial importance plastic that has been investigated by a great number of researchers.[1] However, only a few studies have been concerned with the rheological behavior of the polymerization. Apart from its importance for understanding the reactor design (e.g., agitation, mixing, and heat transfer, etc.), the rheological behavior of the polymerizing system bears a direct relation to many unique phenomena and characteristics of the HIPS prepolymerization, such as phase inversion, the Wessenberg effect, morphology, and particle size variation of the rubber dispersion.

Earlier studies[2,3] concerning the rheological behavior of the HIPS polymerizing system were limited to qualitative descriptions of the rheological anomalies, i.e., the sudden drop in the viscosity and the disappearance of the Wessenberg effect during the phase inversion. Freeguard[4] established that the HIPS polymerizing mass is a pseudoplastic fluid and can be described by the power law equation with the flow behavior index $n < 1$:

$$\tau = K\dot{\gamma}^n \tag{1}$$

Moreover, the maximum departure from Newtonian behavior occurs at the phase inversion point, when the flow behavior index, n, passes through a minimum while the consistency index, K, passes through a maximum. The remarkable non-Newtonian behavior occurs as a consequence of the two-phase nature of the prepolymerizing system. Freeguard also utilized an emulsion viscosity equation to correlate the viscosity of the prepolymerizing system with its two phase viscosities. His work, however, was limited to the simulated system; moreover, the rheological behavior of the simulated polystyrene (PS) phase and rubber (R) phase of his study was not reported. The two phase viscosities—and especially their ratio, $\eta R/\eta_{PS}$—are very important in controlling rubber particle size and also the phase inversion.

This paper presents new experimental data on the rheological behavior

Journal of Applied Polymer Science, Vol. 32, 3349–3369 (1986)
 CCC 0021-8995/86/023349-21$04.00

of the HIPS prepolymerizing system and its two phases separated by ultracentrifugation, and shows the effects of rubber molecular weight (MW), agitation speed, and temperature on the rheological behavior of the prepolymerizing system. The rheological behavior of the separated R phase and the PS phase is also reported. And finally, the viscosity of the prepolymerizing system is correlated to the viscosities of its two phases.

EXPERIMENTAL

Materials

Materials are listed in Table I.

TABLE I

Polybutadiene rubber	*cis*-1,4, 98%. $M_v \times 10^{-4}$:19.24, 24.39, 37.14
Styrene	Polymerizing grade; purified by passage through an ion-exchange column
Benzoyl peroxide (BPO)	C.P. recrystallized
Dicumyl peroxide (DCP)	C.P. recrystallized
N-Dodecyl mercaptan (NDMC)	78%

The viscosity-average molecular weights M_v were determined on the Ubbelodhe viscometer at 30°C, using the following equation:

$$[\eta] = 3.05 \times 10^{-4} M_v^{0.725} \quad (2)$$

Polymerization

Bulk polymerization was carried out in jacketed reactors of either 1-L capacity equipped with an anchor agitator, or of 2-L capacity equipped with a helical ribbon agitator. The rubber concentration was 7 wt % for all runs. Table II presents the polymerization conditions for three typical runs.

Conversion and Polymer Concentrations of Separated Phases

During the reaction courses, samples were withdrawn at given intervals from the reactor, and a small amount of benzoquinone was added to terminate the polymerization. The conversion and the polymer weight concentrations of R and PS phases, separated by the following procedure, were determined by an evaluation of total solids.

TABLE II
Polymerization Conditions

Run	Temperature (°C)	Recipe	Agitation speed (rpm)	Reactor (L)
C	Before PI[a] 80	0.16% BPO + 0.05% DCP	300	1
G	After PI[a] 85	+0.05% NDMC	250	2
H	After PI[a] 112	0.05% DCP + 0.05% NDMC	300	2

[a] PI = phase inversion.

Separation of R and PS Phases

The samples were separated into R and PS phases by the 80P-7 Hitachi ultracentrifuge at a speed of 60,000 rpm, with a centrifugal force of up to 250,000 g for 4 h. After separation, the centrifugal tube was marked outside at the phase interfaces and calibrated with distilled water at 25°C by titration to determine the PS-phase volume. The R-phase mass (upper layer) and the PS-phase mass (lower layer) were removed for determinations of their polymer weight concentrations (C_{PS}, C_R) and $\tau-\dot{\gamma}$ relationships. From the obtained C_R, C_{PS}, and ϕ_{PS}, the degree of rubber grafting, E, can be calculated according to eq. (3):

$$\mathrm{E} = \frac{\text{weight of PS grafted}}{\text{weight of original rubber}} = \frac{(1 - \phi_{PS})C_B - 0.07}{0.07} \tag{3}$$

Measurement of Rheological Behavior

The shear rate $\dot{\gamma}$ – shear stress τ relationships of the polymerizing system and its separated two phases were measured at 30°C by the cone-and-plate system of the Rheotest-2 viscometer. The concentric rotating cylinder system of the RHEOTEST-2 was used to measure the temperature dependence of rheological behavior.

Molecular Weight Measurement

The number-average molecular weight (M_n) and weight-average molecular weight (M_w), as well as the molecular weight distribution of the free PS, were determined by measuring the dried samples of PS phase in the NA-2 Gel Permeation Chromatograph at 26°C, using tetrahydrofuran as a solvent.

RESULTS AND DISCUSSION

Rheological Characteristics of the HIPS Prepolymerizing System

The experiments confirm that the HIPS prepolymerizing system is a pseudoplastic fluid and can be described by eq. (1). Therefore, the apparent viscosity, η_a, of the system can be calculated by the following equation:

$$\eta_a = K\,\dot{\gamma}^{n-1} \tag{4}$$

Effect of Rubber MW and the First Minimax Point

At constant agitation speed (240 rpm), the variations of apparent viscosity (η_a), flow behavior index (n), and consistency index (K) of the prepolymerizing systems having different rubber molecular weights with conversion (X) are shown in Figures 1–3, respectively. All systems are pseudoplastic

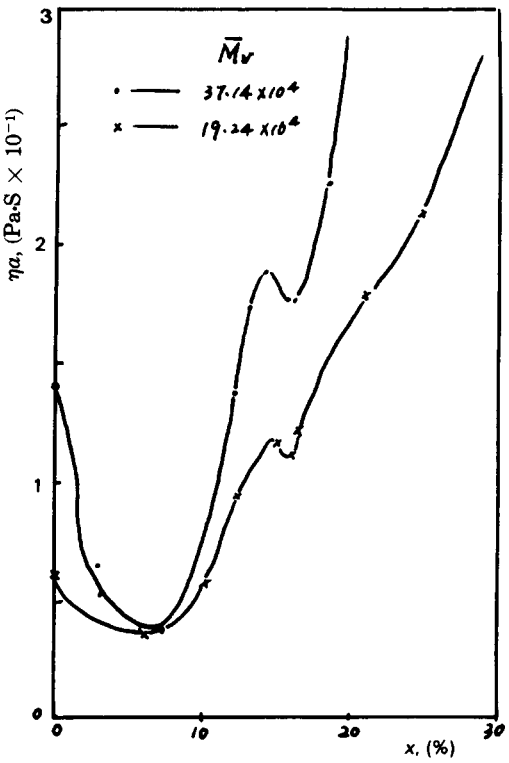

Fig. 1. Variation of prepolymer apparent viscosity with conversion, 30°C.

($n < 1$), and the greater the rubber M_v, the stronger the pseudoplastic behavior and the higher the apparent viscosity of the system. It is important to note that two minimax points exist on each of the curves in the three figures, and these minimax points correspond to each other. The second minimax point lies at about 15% conversion and is generally reported in the literature as the phase inversion point. On the other hand, the first minimax point lies at about 7% conversion and was not reported previously. The existence of the first minimax point is further confirmed by the agitation power versus conversion curve (Fig. 4), which is essentially the variation in apparent viscosity of the system with conversion at the polymerization temperature. The first minimax point, unlike the phase inversion point, is obtained from a progressive variable process. It is caused by the two-phase nature of the system. Before polymerization, the molecular chains of rubber in styrene (which is a good solvent) are fully stretched and give the system a comparably high viscosity. However, when PS is produced at the start of the polymerization, the initially stretched rubber chains begin to curl up, owing to the incompatibility of rubber and PS,[1] thus causing a decrease in the viscosity of the system. The system viscosity is further decreased when phase separation takes place. The appearance and the size of the PS-phase dispersion droplets are the main factors causing the decrease in the system viscosity. The viscosity of the heterogeneous system is determined by the rheological contributions of both the continuous and dispersive phases. The viscosity of the PS phase is much lower than

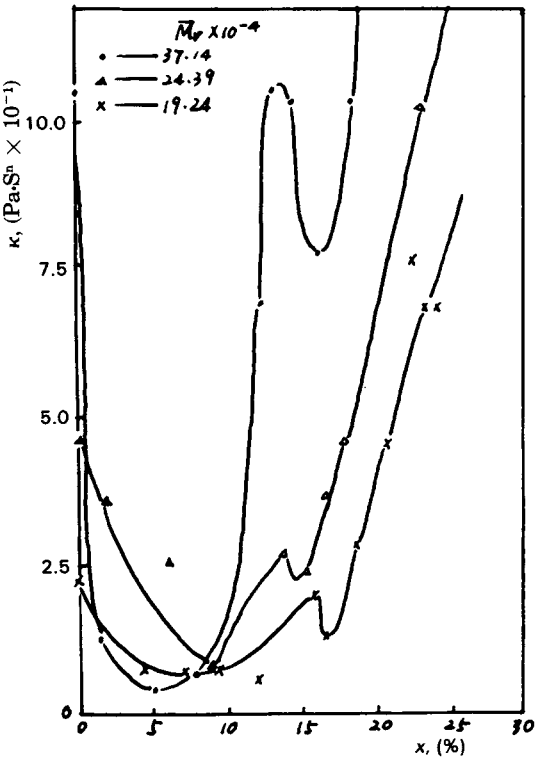

Fig. 2. Variation of prepolymer consistency index K with conversion X, 30°C.

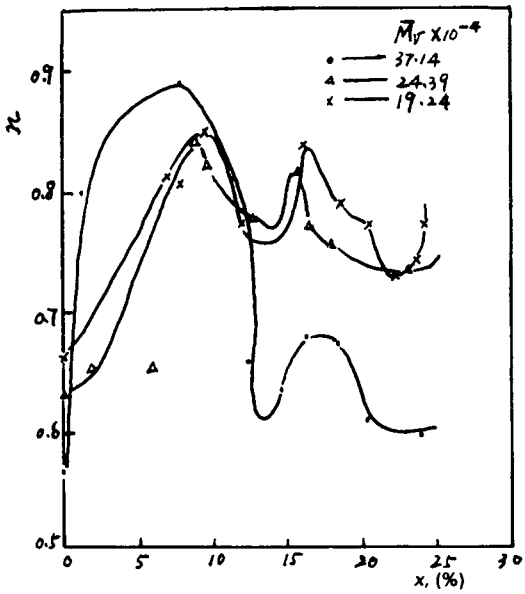

Fig. 3. Variation of prepolymer flow behavior index n with conversion X, 30°C.

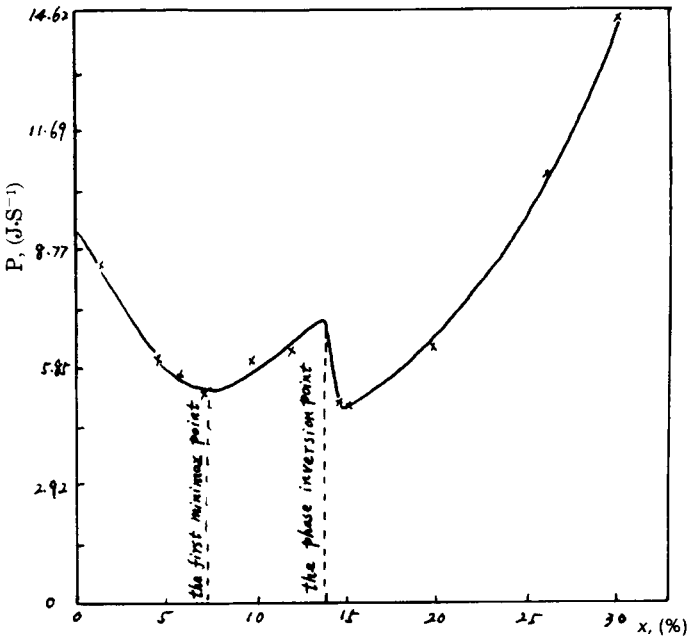

Fig. 4. Variation of agitation power P with conversion X at 112°C.

that of the R phase. For water–oil emulsion systems, Becher[6] reported that an increase in dispersion droplet size and distribution causes the emulsion viscosity to decrease. The same effect holds for poo emulsion systems. In contrast, the concentrated effect of the R phase tends to increase the system viscosity. Therefore, the occurrence of the first minimax point is the result of competition between the two opposing effects. Before the first minimax point, the effect of decreasing viscosity dominates over the concentrated effect whereas beyond the minimax point, the latter begins to prevail.

The Effect of Agitation Speed

In order to determine the influence of agitation speed on the rheological behavior of the polymerizing systems, four different speeds were employed. The results are given in Figures 5–7. Figure 5 shows that the polymerizing system with a high agitation speed presents a lower apparent viscosity, due to the structural change in the poo emulsion. A higher agitation speed tends to increase coalescence between the newly produced PS-phase dispersed droplets and thus causes the increase in the dispersed droplet size and the size distribution; thus the viscosity of the obtained prepolymerizing mass will be lowered. The effect of agitation speed on the consistency index, K, is similar to its effect on the apparent viscosity. However, the effect of agitation speed on the flow behavior index, n, is somewhat complicated. It appears that the higher agitation speed produces systems with a lower n before phase inversion, but a higher n after phase inversion. This indicates the different functions of agitation speed before and after phase separation.

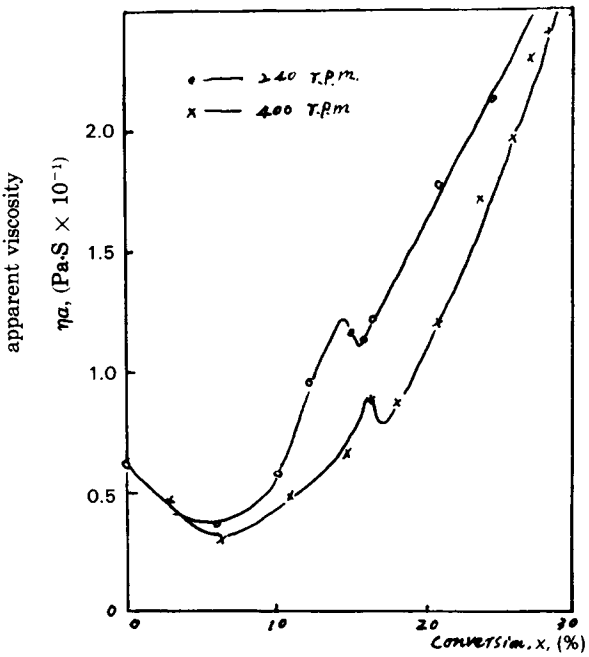

Fig. 5. Effect of agitation speed on the apparent viscosity, η_a, $\overline{M}_r = 19.24 \times 10^4$.

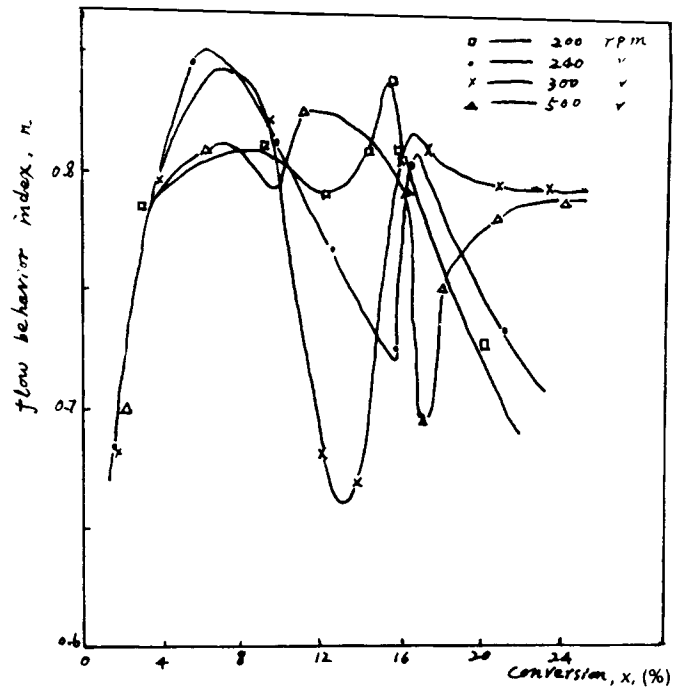

Fig. 6. Effect of agitation speed on the flow behavior index n, $\overline{M}_v = 19.24 \times 10^4$.

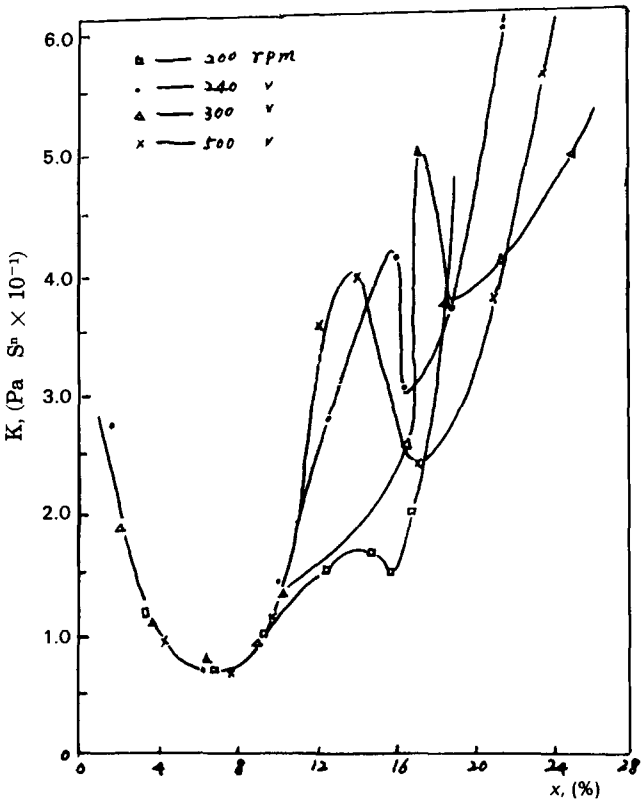

Fig. 7. Effect of agitation speed on the consistency index, K.

Effect of Temperature

The viscosity of the final prepolymer is important for industrial production and reactor design. Therefore, the rheology–temperature relationship of prepolymers with different conversions (X = 25–32%) was studied. In order to ensure comprehensive understanding, the rheology–temperature data of the polymerizing mass before phase inversion ($X \leq 14.8\%$) and the simulated solution of 16% conversion prepolymer were also measured.

Figures 8 and 9 show the influences of temperature on K and n, respectively. As the temperature is increased, K decreases whereas n increases slightly. Such temperature dependence was also reported for other non-Newtonian fluids.[9]

For many fluids, the relation of viscosity to temperature can be expressed by the following equation:

$$\eta = \eta_0 \exp(E_v/RT) \tag{5}$$

where E_v is known as the flow activity energy. When ln η_a is plotted against $1/T$, a straight line can be obtained for the HIPS prepolymers, indicating agreement with eq. (5). (Fig. 10). However, because of non-Newtonian behavior of this system, the straight lines vary with shear rate. In fitting the

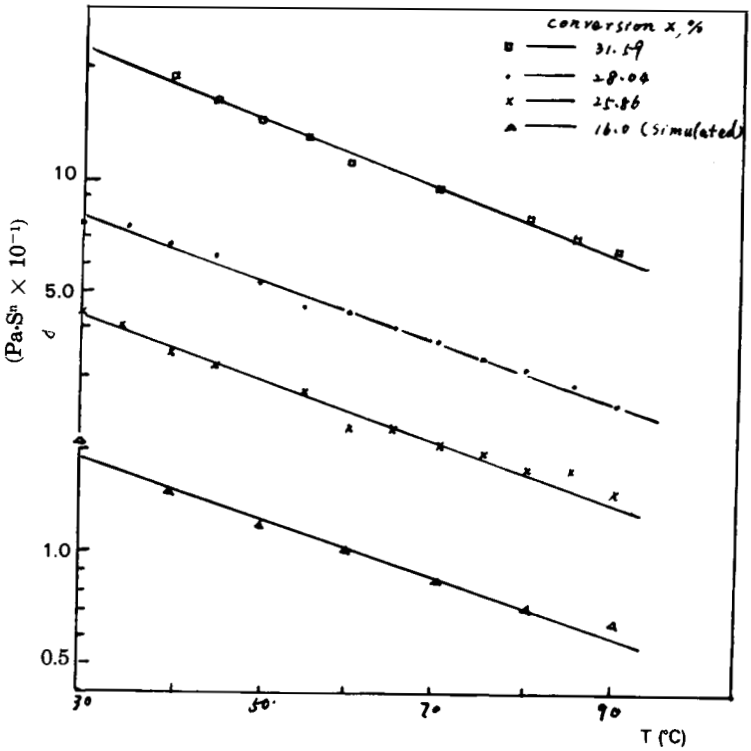

Fig. 8. Effect of temperature on the consistency index, K.

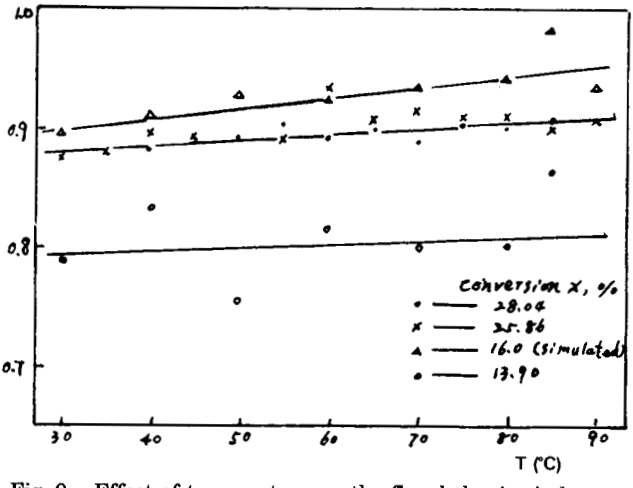

Fig. 9. Effect of temperature on the flow behavior index, n.

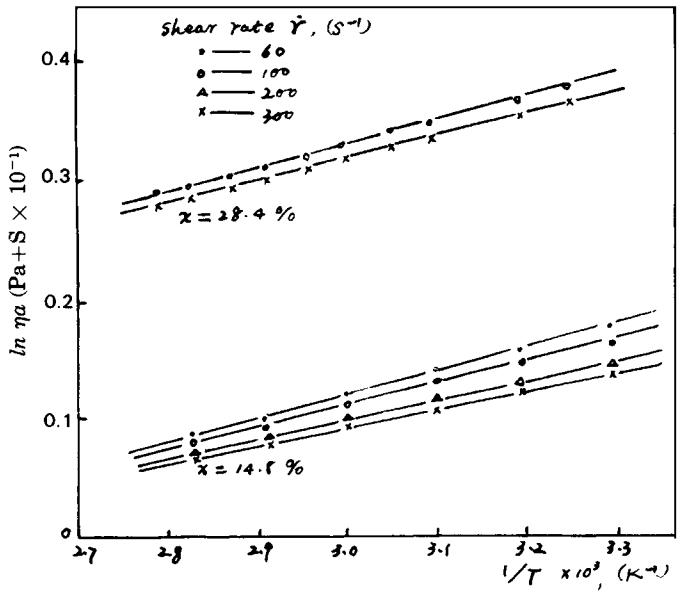

Fig. 10. Effect of temperature on the apparent viscosity, η_a.

experimental data to eq. (5), η_0 and E_v/R of eq. (5) had an exponential relation with shear rate $\dot{\gamma}$. Consequently, eq. (5) can be written as:

$$\eta_a = B_2\,\dot{\gamma}^{A2}\exp[(B_1\dot{\gamma}^{A1})/T] \tag{6}$$

Table III presents the values of A_1, A_2, B_1, and B_2 for prepolymers at different conversions. The relative deviation of eq. (6) does not exceed 5%.

Rheological Behavior of R Phase and PS Phase

Rheological Behavior of the PS Phase

The measured results for the PS phase are shown in Table IV and illustrated in Figure 11. The PS phase shows Newtonian behavior until 17% conversion, after which it begins to show pseudoplastic behavior, with n decreasing and η_{PS} rising dramatically as conversion is raised. The viscosity values after 17% conversion (Fig. 11) are calculated for a shear rate of 100 s^{-1}.

TABLE III
Regressive Coefficient of Equation (6)[a]

Conversion X%	14.80	16.0 (simulated)	25.86	28.04	31.59
A_1	-0.1866	-0.03871	-0.03439	-0.02365	-0.07695
B_1	4365	2215	2006	2171	2495
A_2	0.8213	0.1371	0.07362	0.0310	0.2701
B_2	2.575	143.8	631.0	679.9	990.6

[a] 60 $s^{-1} \le \dot{\gamma} \le$ 500 s^{-1}; 30°C ≤ I ≤ 90°C

TABLE IV
Properties of the PS Phase at 30°C

	X %	1.51	4.44	5.85	7.30	9.88	12.25	14.32	15.31	20.08	26.60
	Measured	0.3859	0.4305	0.4873	0.5424	0.6979	0.9811	1.492	1.883	18.25	47.81
	Eq. (8)	0A358	0.4407	0.3984	0.4851	0.6521	0.8981	1.244	1.600	—	—
Run	η	1	1	1	1	1	1	1	1	0.822	0.800
H	C_{ps}	0.1233	0.1509	0.1675	0.1851	0.2052	0.2316	0.2629	0.2754	0.3264	0.3726
	$M_w \times 10^{-4}$	28.9	19.3	14.5	14.2	13.7	13.5	13.2	14.4	16.6	16.9
	M_w/M_n	1.91	2.11	2.15	2.08	2.20	2.01	2.17	2.18	2.26	2.17
	X %	4.24	6.25	8.47	12.50	14.72	16.33	17.34			
	Measured	0.2174	0.4123	0.4663	0.8050	1.208	1.502	2.036			
	Eq. (8)	0.2240	0.3886	0.5905	0.9393	1.256	1.445	1.599			
Run	η	1	1	1	1	1	1	1			
G	C_{ps}	0.1585	0.1945	0.2278	0.2662	0.2898	0.3033	0.3130			
	$M_w \times 10^{-4}$	10.7	10.5	10.3	10.5	10.9	11.0	11.1			
	M_w/M_n	1.73	1.94	1.91	2.06	2.03	2.25	2.30			
	X %	1.78	4.39	7.73	10.10	14.66	15.14	15.71			
	Measured	0.2237	0.3007	0.3084	0.4286	1.076	1.172	1.450			
	Eq. (8)	—	0.2658	0.3317	0.4912	1.422	1.191	1.713			
Run	η	1	1	1	1	1	1	1			
C	C_{ps}	0.1228	0.1536	0.1797	0.2048	—	0.2628	0.2893			
	$M_w \times 10^{-4}$	—	12.9	11.0	11.2	13.9	12.8	13.7			
	M_w/M_n	—	2.19	2.18	2.11	2.25	2.06	2.45			

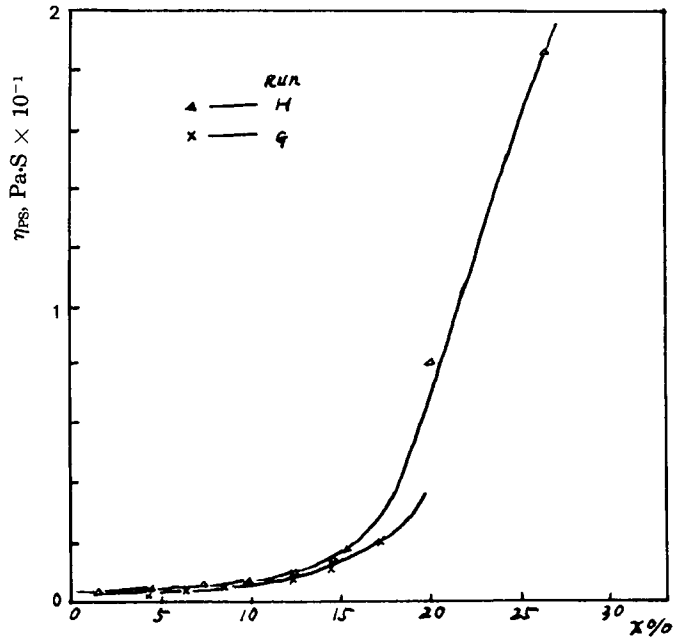

Fig. 11. PS phase viscosity η_{PS} in the course of prepolymerization, 30°C.

Computer programs were developed to fit experimental data to the power equation by means of the least-squares procedure. Thus, eq. (8) was obtained for the PS phase:

$$\eta_{PS} = 1.516\, C_{PS}^{2.81}\, M_w^{1.38} \tag{8}$$

The viscosity values calculated by eq. (8) are also shown to be comparable to the experimental data (see Table IV).

Rheological Behavior of the R phase

The measured results of the R phase are presented in Table V. The R phase, like the prepolymer, is pseudoplastic. The variations of η_r, K_R, and n_R with conversion are plotted in Figures 12–14. Both K_R and η_R increase with conversion, and all data from the different runs fall on the same curve, which shows the independence of the polymerizing conditions. In contrast to the K_R and η_R, n_R decreases with increasing conversion, which indicates the increasingly non-Newtonian behavior of the R phase. Because of the higher grafting degree of runs G and C, their R phases present stronger pseudoplastic behavior and have smaller n values (Fig. 14).

Because the viscosity of the R phase depends on shear rate, it is difficult to correlate the rheological data. However, the difficulty can be overcome by the following treatment. For the constant $\dot{\gamma}$, assume that the apparent viscosity of the R phase has the form:

$$\eta_R(\dot{\gamma}) = AE^a\, C_R^b \tag{9}$$

TABLE V
Properties of the R Phase at 30°C

	X %	1.51	4.44	5.85	7.30	9.88	12.25	14.22	15.31	20.08
	$K_R(P \cdot S^{1-n})$	17.49	41.72	65.25	116.4	256.3	347.2	566.8	633.7	1225
Run	n_R	0.7485	0.7060	0.6874	0.6142	0.563	0.5448	0.5294	0.5158	0.5020
H	C_R	0.08396	0.1025	0.1187	0.1281	0.1508	0.1751	0.1936	0.2024	0.2456
	E	0.0179	0.1248	0.1354	0.1818	0.2829	0.3421	0.3948	0.4174	0.5920
	X %	4.237	6.25	8.47	14.72	16.33	17.34			
	$K_R(P \cdot S^{1-n})$	53.12	140.9	190.7	553.0	887.0	915.0			
Run	n_R	0.6950	0.5774	0.5503	0.5127	0.5034	0.5028			
G	C_R	0.1137	0.1468	0.1707	0.2146	0.2269	0.2360			
	E	0.2005	0.2572	0.3614	0.6096	0.6661				
	X %	1.782	4.385	7.73	10.10	12.58	14.66	15.14		
	$K_R(P \cdot S^{1-n})$	21.77	40.16	100.2	176.8		342.6	505.8		
Run	N_R	0.7095	0.6959	0.6308	0.5523		0.5270	0.5153		
C	C_R	0.08675	0.1089	0.1354	0.1576	0.1804	0.1972	0.2068		
	E	0.1055	0.1988	0.3100	0.4557	0.5491	0.5781			

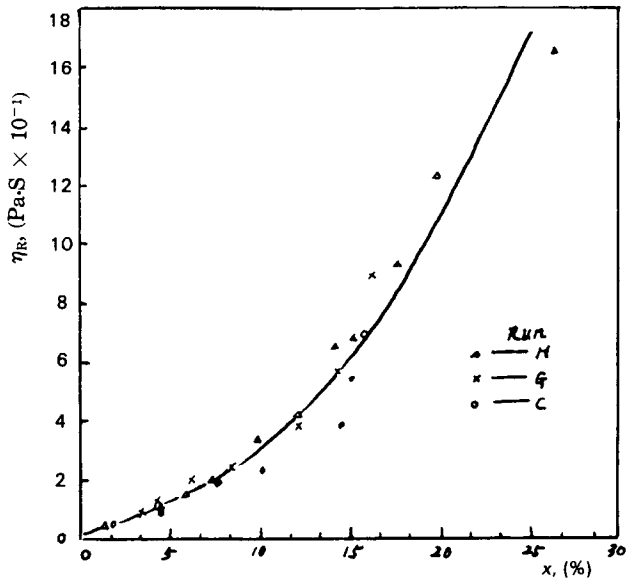

Fig. 12. Rubber phase viscosity η_R in the course of prepolymerization, 30°C.

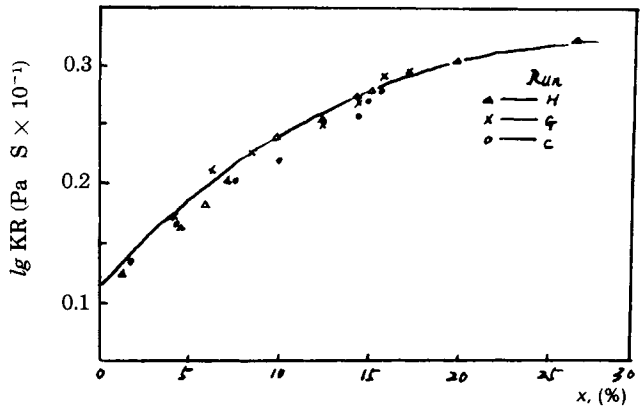

Fig. 13. Consistency index of the R phase in the course of prepolymerization, 30°C.

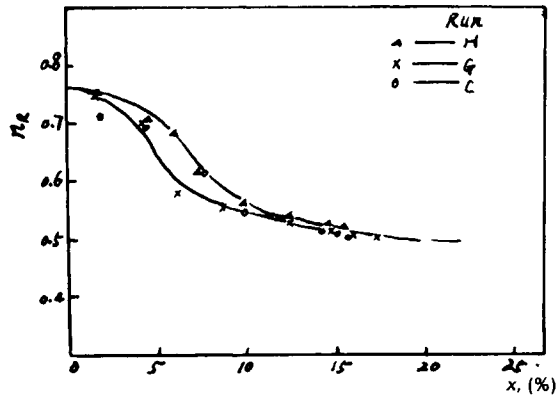

Fig. 14. Flow behavior index of the R phase in the course of prepolymerization, 30°C.

The constants A, a, and b are then related to the shear rate, $\dot{\gamma}$. The entire procedure was performed on a computer using the least-squares method to obtain the following regressive equations:

$$\eta_R = 3.595 \times 10^5 \, \dot{\gamma}^{-0.862} E^a C_R^b \tag{10}$$

where $a = -(0.1139 + 0.00648 \ln \dot{\gamma})$ (10a)

$b = 4.126 + 0.2376 \ln \dot{\gamma}$ (10b)

Viscosity Ratio of the Two Phases

Figure 15 shows the dependence of the viscosity ratio of the two phases, η_R/η_{PS}, on conversion. There is a great difference in viscosity between the R phase and the PS phase. Before phase inversion, the η_R/η_{PS} ratio can reach the value of about 60. After phase inversion, it decreases with increasing conversion because the PS phase begins to exhibit non-Newtonian behavior, and its apparent viscosity increases sharply. The free polystyrene molecular weight, and thus its viscosity (η_{PS}), for runs C and G are lower than that for run H. Consequently, the η_R/η_{PS} is greater for runs C and G than for run H. As illustrated in Figure 15, the η_R/η_{PS} decreases with increasing shear rate. This is expected from the equation:

$$\frac{\eta_R}{\eta_{PS}} = \frac{K_R}{K_{PS}} \cdot \dot{\gamma}^{\eta_R - \eta_S} \tag{11}$$

since $\eta_R < \eta_{PS}$. Significantly, the ratio enables us to control the rubber particle size and particle size distribution through regulation of the agitation speed. The η_r/η_{PS} can be calculated from eqs. (8) and (9) as follows:

$$\frac{\eta_R}{\eta_{PS}} = 2.371 \times 10^5 \, \dot{\gamma}^{-0.862} M_w^{-1.38} C_{PS}^{-2.81} E^a C_R^b \tag{12}$$

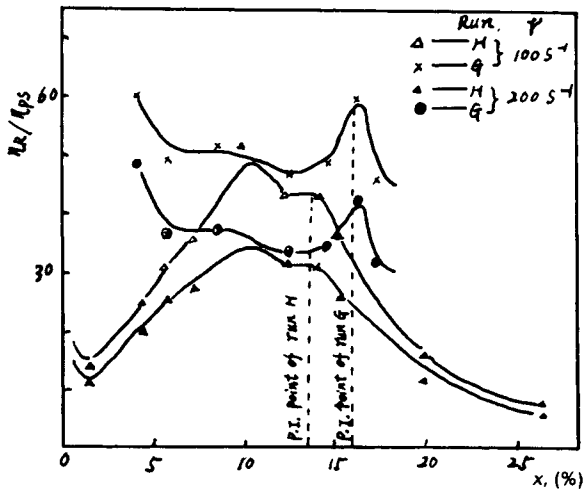

Fig. 15. Viscosity ratio of the R phase and PS phase in the course of prepolymerization, 30°C.

Correlation of the Prepolymerizing System Viscosity with Its Two Phase Velocities

For water–oil emulsions, there have been many equations correlating the system viscosity with its two phase viscosities.[4,6]

$$\eta = \eta_c (1 + 2.5\phi + A\ \phi^2 + B\ \phi^3) \qquad A = 4 \sim 10 \tag{13}$$

$$\ln(\eta/\eta_c) = A\ \phi/(1 - B\ \phi) \qquad A = 2.5, B = 1.35 \tag{14}$$

$$\eta = \eta_c \exp(B\ \phi) \tag{15}$$

$$\eta = \eta_c/(1 - \phi^B) \qquad B = 1/3 \tag{16}$$

$$\eta = \eta_c\ [1 + B\ \phi\ (\eta_d + A\ \eta_c)/(\eta_d + \eta_c)] \qquad A = 0.4, B = 2.5 \tag{17}$$

$$\lg(\frac{\eta}{\eta_c}) = \frac{B[(\eta_d + A\eta_c)]}{(\eta_a + \eta_c)}(\phi + \phi^{5/3} + \phi^{\frac{11}{3}}) \qquad B = 2.5 \tag{18}$$

Where A and B are constants that can be adjusted during fitting. The A,B values are usually given for water–oil emulsion systems. By fitting the data of the simulated solution to the above equations, Freeguard[4] found that eq. (18) was the best equation to fit the data before phase inversion, where the A value was −0.505. However, eq. (18) does not fit well our experimental data obtained by direct separation of the HIPS prepolymer into two phases, in contrast to its simulated solution. For this reason, we have derived the following equation based on an alternative model:

$$\frac{1}{\eta} = \frac{\mathrm{A}(1-\phi_{PS})}{\eta_R + B(\phi_{PS}/\eta_{PS})} \tag{19}$$

This equation, together with eqs. (13) to (18) were fitted to our experimental data on a computer to find out the best model equation and its parameters. During fitting, the mean relative deviation was defined as:

$$(DEF) = \sum_{i=1}^{P_0} \frac{(\eta_i - \eta_i)^2/\eta_i^2}{P_0} \tag{20}$$

where η_i and η_i are viscosities measured and calculated from the fitting model equation, respectively, and P_0 is the number of fitting points. By adjusting A and B values to minimize (DEF), the best model equation could be chosen. The result is shown in Table VI. As illustrated in Table VI, eq. (19) is the best equation to fit the experimental data before phase inversion.

TABLE VI
The Optimized Regressive Coefficients and (DEF) of eqs. (13) to (19)

Equation	(13)	(14)	(15)	(16)	(17)	(18)	(19)
A	4	18	—	—	−0.60	−0.505	0.696
B	−3000	15	−5	1/3	4.5	2.5	0.311
(DEF)%	$>2\ 10^6$	22.63	8.31	15967	30.49	11.24	4.02

This result is clearly shown in Figure 16. By the same fitting procedure, $A = 6.098$ and $B = 0.166$ were obtained for eq. (19) after phase inversion. Thus, eq. (19) can be used to predict the prepolymer viscosity for the whole prepolymerization period (Fig. 17). A similarly good fit can be obtained for viscosities in the shear-rate range from 60 to 500 s^{-1}.

Equation (19) is derived from an alternative model. Assume that there are N kinds of incompatable fluids having different viscosities regularly and concentrically distributed into N adjacent layers in a gap between outer and inner cylinders, the radii of which are R_b and R_c, respectively, of a concentrically rotating cylinder viscometer (Fig. 18). As the outer cylinder rotates, each layer of fluids in the gap follows one after another to cause laminar flow. The viscosity of the fluid of the layer whose inner and outer radii are R_{i-1} and R_i is η_i. At a static state, the torque (M) in the gap is everywhere uniform so that:

$$M = 2\pi h R_b^2 \tau_b = 2\pi h R_i^2 \tau_1 = \ldots = 2\pi h R_i^2 \tau_i = \ldots = 2\pi h R_c^2 \tau_c \quad (21)$$

Therefore,

$$\tau_i = \frac{M}{2\pi h R_i^2} \quad (22)$$

According to the basic equation for a concentrically rotating cylinder viscometer:[9,10]

$$\Omega = -\frac{1}{2}\int_{\tau_i}^{\tau_b} \frac{\dot{\gamma}(\tau)}{\tau} d\tau \quad (23)$$

where Ω is the angular velocity of the outer cylinder. For a Newtonian fluid where $\dot{\gamma}(\tau)/\tau = \frac{1}{\eta}$ is constant, the equation can be obtained by sub-

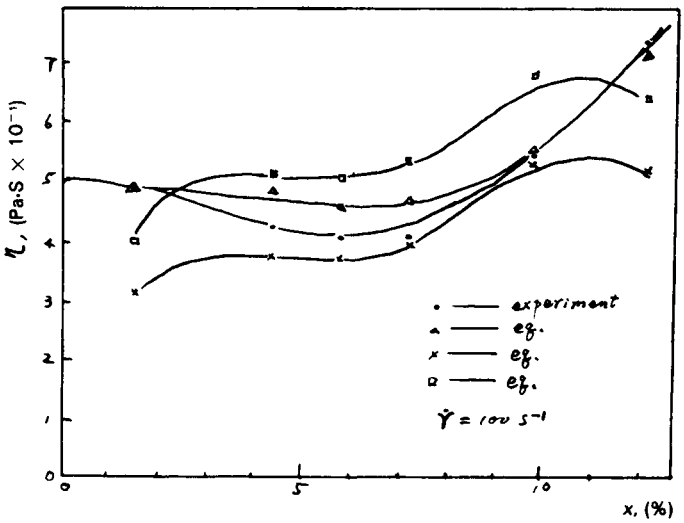

Fig. 16. Comparison of calculated viscosities with the measured value.

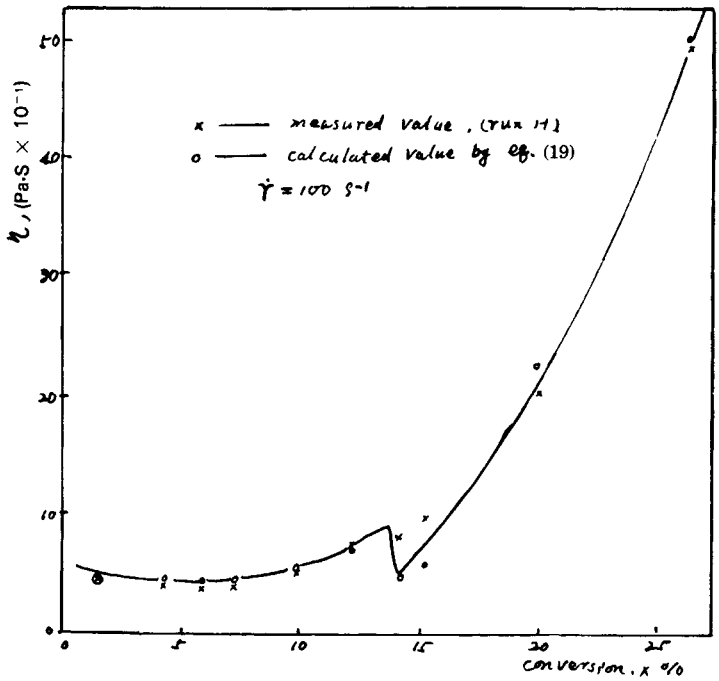

Fig. 17. Comparison of the calculated viscosity value from eq. (19) with the measured value obtained during the entire prepolymerization.

stituting eq. (22) in eq. (23):

$$\Omega = \frac{1}{2} \cdot \frac{M}{2\pi h} \cdot \sum_{i=1}^{N} \frac{(1/R_{i-1}^2) - (1/R_i^2)}{\eta_i} \tag{24}$$

When $N = 1$, that is, when only one kind of fluid with viscosity η is in the gap, eq. (24) is reduced to:

$$\Omega = \frac{1}{2} \cdot \frac{M}{2\pi h} \cdot \frac{(1/R_b^2) - (1/R_c^2)}{\eta} \tag{25}$$

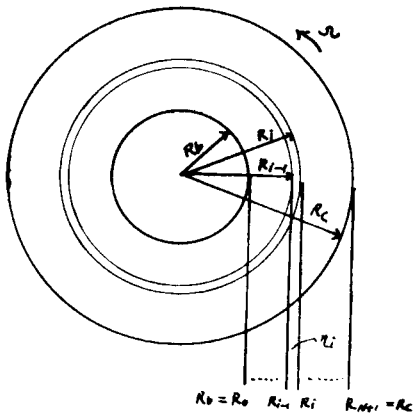

Fig. 18. Polylaminate model in concentrically rotating cylinders.

The effective or equivalent viscosity of the above polylaminate fluids is then defined as the viscosity of the single homogeneous fluid which, when measured in the same rotating cylinder viscometer, will give the same torque M to the inner cylinder at the same angular velocity of the outer cylinder as the polylaminate fluids do. Thus, by comparing eqs. (24) and (25), the following equation can be obtained:

$$\frac{1}{\eta} = \frac{R_b^2 R_c^2}{R_c^2 - R_b^2} \cdot \sum_{i=1}^{N} \frac{(1/R_{i-1}^2) - (1/R_i^2)}{\eta_i} \tag{26}$$

In the special case where only two kinds of fluids with viscosities η_1 and η_2 are alternatively distributed in the gap, the above equation is reduced to:

$$\frac{1}{\eta} = \frac{R_b^2 R_c^2}{R_c^2 - R_b^2} \left(\sum_{i=0}^{N} \frac{(-1)^i / R_i^2}{\eta_1} + \sum_{i=1}^{N+1} \frac{(-1)^{i+1} / R_i^2}{\eta_2} \right) \tag{27}$$

which again can be simply written as

$$\frac{1}{\eta} = \frac{\alpha}{\eta_1} + \frac{B}{\eta_2} \tag{(28)}$$

where α and β are obviously functions of the volume fraction of the two fluids. A similar form of eq. (28) can also be derived in a cone-and-plate viscometer or a capillary viscometer for the alternative polylaminate layer model. If we let α and β be proportional to the phase volume function, then eq. (28) becomes eq. (19).

CONCLUSIONS

1. As the polymerization proceeds, the apparent viscosity of HIPS prepolymerizing mass initially decreases, passing through a minimum at about 7% conversion, and then rises normally until phase inversion, when the apparent viscosity of the system drops suddenly.

2. The rheological behavior of the HIPS prepolymer is influenced by rubber molecular weight, agitation speed, and temperature. With higher rubber molecular weight, the system presents stronger pseudoplastic behavior and high apparent viscosity. With higher agitation speed, the apparent viscosity of the obtained polymerizing system is smaller. A rise of temperature, on the other hand, will cause the apparent viscosity and consistency index of the prepolymerizing system to decrease and the flow behavior index to increase slightly. The apparent viscosity of the prepolymer can be well correlated in eq. (6) with temperature and shear rate.

3. Before about 17% conversion, the PS phase of the HIPS prepolymerizing mass shows Newtonian behavior, the viscosity of which can be determined by eq. (8); whereas at higher conversion, the PS phase begins to show pseudoplastic behavior, with the apparent viscosity rising dramatically and the flow behavior index decreasing as the conversion increases.

4. During the whole period of prepolymerization, the R phase is pseudoplastic and its apparent viscosity can be determined by eq. (10).

5. The apparent viscosity of the R phase is much greater than that of the PS phase, and, because there is a difference in the extent of pseudoplastic behavior of the two phases, the viscosity ratio of the two phases, η_R/η_{PS}, which varies with conversion, can be regulated through the change in agitation speed.

7. Equation (19) was derived from an alternative polylaminate model correlating the system viscosity to its two phase viscosities. It fits the experimental data much better than the other six equations proposed previously.

Nomenclature

A, A_1, A_2, B, B_1, B_2	Constants
a, b	Function of shear rate defined by eqs. (10a) and (10b)
c	Weight percent concentration
E	Degree of rubber grafting
E_v	Flow activity energy, J·mol^{-1}
h	Height of inner cylinder immersed by fluids, cm
K	Consistency index, Pa·S^{n-2}
M	Torque, dyn·cm
M_n, M_w, M_v	Number, weight, and viscosity average molecular weight, respectively
N	Number of layers
n	Flow behavior index
p	Power, J·S^{-1}
P_0	Number of points fitted
R	Gas constant, J·K^{-1} · mol^{-1}
R_b, R_c	Radii of inner and outer cylinders, respectively, cm
T	Temperature, K
X	Conversion
α,β	Constants
$\dot{\gamma}$	Shear rate, s^{-1}
τ	Shear stress, dyn·cm^{-2}
η	Viscosity, Pa·S
η_0	Coefficient of eq. (5)
Ω	Angular velocity, s^{-1}

Subscripts Used

a	Apparent
b	Inner cylinder
c	Outer cylinder
PS	PS phase
R	R phase

References

1. C. B. Bucknall, *Toughened Plastics*, 1977.
2. B. W. Bender, *J. Appl. Polym. Sci.*, **9**, 2887 (1965).
3. G. E. Molau, *J. Appl. Polym. Sci.*, **13**, 2735 (1969).
4. G. F. Freeguard, *J. Appl. Polym. Sci.*, **15**, 1649 (1971).
5. J. Brandrup, *Polymer Handbook* 2nd Ed., 1975.
6. P. Becher, *Emulsions—Theory and Practice, 1957.*
7. D. W. Van Krevelen, *Properties of Polymers*, 1976.
8. R. Kruse, *J. Rheol.*, **24**(6), 755 (1980).
9. Nanjing Chemical Engineering College, Ed., *Processes and Equipment of Polymerization*, 1980.
10. Van Wazer, *Viscosity and Flow Measurement*, 1963.

Received March 1, 1985
Accepted July 3, 1985